PROCEEDINGS OF SCIENCE

FERMILAB-CONF-25-0051-T
MITP-25-008
TUM-EFT 195/25

Strong coupling in (2+1+1)-flavor QCD

Viljami Leino,[a,b,*] **Alexei Bazavov,**[c] **Nora Brambilla,**[d,e,f] **Andreas S. Kronfeld,**[g,f] **Julian Mayer-Steudte,**[d,e] **Peter Petreczky,**[i] **Sebastian Steinbeißer,**[d,j] **Antonio Vairo**[d] **and Johannes H. Weber**[k,l]

[a] *Helmholtz Institute Mainz, Staudingerweg 18, 55128 Mainz, Germany*
[b] *Institut für Kernphysik, Johannes Gutenberg-Universität Mainz, Johann-Joachim-Becher-Weg 48, 55128 Mainz, Germany*
[c] *Department of Computational Mathematics, Science and Engineering, and Department of Physics and Astronomy, Michigan State University, East Lansing, Michigan 48824, USA*
[d] *Physics Department, TUM School of Natural Sciences, Technical University of Munich, James-Franck-Straße 1, 85748 Garching b. München, Germany*
[e] *Munich Data Science Institute, Technical University of Munich, Walther-von-Dyck-Straße 10, 85748 Garching b. München, Germany*
[f] *Institute for Advanced Study, Technical University of Munich, Lichtenbergstraße 2a, 85748 Garching b. München, Germany*
[g] *Particle Theory Department, Theory Division, Fermi National Accelerator Laboratory, Batavia, Illinois 60510-5011, USA*
[i] *Physics Department, Brookhaven National Laboratory, Upton, New York 11973-5000, USA*
[j] *Leibniz-Rechenzentrum der Bayerischen Akademie der Wissenschaften, Boltzmannstraße 1, 85748 Garching b. München, Germany*
[k] *Institut für Physik & IRIS Adlershof, Humboldt-Universität zu Berlin, Zum Großen Windkanal 2, D-12489 Berlin, Germany*
[l] *Institut für Kernphysik, Technische Universität Darmstadt, Schlossgartenstraße 2, D-64289 Darmstadt, Germany*

E-mail: viljami.leino@uni-mainz.de

TUMQCD Collaboration

The strong coupling α_s can be obtained from the static energy as shown in previous lattices studies. For short distances, the static energy can be calculated both on the lattice with the use of Wilson line correlators, and with the perturbation theory up to three loop accuracy with leading ultrasoft log resummation. Comparing the perturbative expression and lattice data allows for precise determination of $\alpha_s(m_Z)$. We will present preliminary results for the determination of $\alpha_s(M_Z)$ in (2+1+1)-flavor QCD using the configurations made available by the MILC-collaboration with smallest lattice spacing reaching 0.0321 fm.

The 41st International Symposium on Lattice Field Theory (LATTICE2024)
28 July - 3 August 2024
Liverpool, UK

*Speaker

1. Introduction

The strong coupling α_s is a fundamental parameter of QCD and the Standard Model of particle physics. The running of the strong coupling in the $\overline{\text{MS}}$ scheme is a function of the renormalization scale μ and the intrinsic scale of QCD, $\Lambda_{\overline{\text{MS}}}$. When $\Lambda_{\overline{\text{MS}}}$ is known, one can perturbatively determine α_s at any scale $\mu \gg \Lambda_{\overline{\text{MS}}}$. In these proceedings we focus on determining this intrinsic scale.

Observables that can be calculated with high precision in both perturbative- and lattice-QCD are ideal candidates to determine α_s in the regions where both approaches agree. One such observable is the energy between a static quark and a static antiquark separated by distance r known as the static energy $E_0(r)$. $E_0(r)$ is a fundamental observable of QCD that played an important role [1] in establishing confinement in QCD and understanding asymptotic freedom. On the lattice, $E_0(r)$ is defined as the ground state of a static Wilson loop. At short distances $r\Lambda_{\overline{\text{MS}}} \ll 1$, it holds that $\alpha_s(1/r) \ll 1$ and the static energy is well defined by a weak coupling perturbative expansion. This expansion is known up to N^3LL level [2–7]. By comparing the perturbative expansion of the static energy to the static energy on the lattice at short distances, we can extract $\Lambda_{\overline{\text{MS}}}$.

So far, $\Lambda_{\overline{\text{MS}}}$ has been determined from the static energy in $N_f = 0$ the pure gauge SU(3) Yang-Mills theory [8–10] and with either $N_f = 2$ dynamical quark flavors [11–13] or with $N_f = 2 + 1$ dynamical flavors [14–18]. With $N_f = 2 + 1 + 1$ dynamical flavors, $\Lambda_{\overline{\text{MS}}}$ via the static energy is yet to be determined, however, $\Lambda_{\overline{\text{MS}}}$ has been determined on the lattice in 2+1+1-flavor QCD with other methods [19, 20]. In these proceedings, we report on the progress of the newest TUMQCD lattice extraction of $\Lambda_{\overline{\text{MS}}}$ from the lattice with 2+1+1 dynamical flavors via the static energy. For a complete review of the status of α_s determined from the lattice QCD, we refer the reader to the recent FLAG review [21] and for a wider review with also the experimental status to Ref. [22].

2. Static energy

2.1 Perturbation theory

The static energy $E_0(r)$ has the perturbative expansion

$$E_0(r) = \Lambda - \frac{C_F \alpha_s}{r}\left(1 + \#\alpha_s + \#\alpha_s^2 + \#\alpha_s^3 \ln \alpha_s + \#\alpha_s^3 + \#\alpha_s^4 \ln^2 \alpha_s + \#\alpha_s^4 \ln \alpha_s + \dots\right), \tag{1}$$

where Λ is a constant of mass dimension one and the coefficients # can be found in the review [23]. The running coupling depends on a soft scale μ that is commonly set to be $\mu = c/r$ with c varied around 1 to gauge perturbative error. Starting at order α_s^4 ultrasoft logarithms are introduced with ultrasoft scale $\nu = C_A \alpha_s(\mu)/2r$. These logarithms can be resummed, however, in these proceedings we show results only without resummation and leave the study of ultrasoft scale dependence to the final publication. The expansion given by Eq. (1) is known to the order given for massless sea quarks. To include the effects from the finite mass of the charm quark, a correction $\delta V_m^{(N_f)}(r)$ has to be added to the static energy. This correction is known in perturbation theory up to order of α_s^3 (see Ref. [24] for summary of equations). With (2+1+1)-flavor QCD, the relevant massive quark is the charm quark that has a mass $m_c^{\overline{\text{MS}}}(m_c^{\overline{\text{MS}}}) \approx 1.28\ \text{GeV} \simeq 1/0.15\ \text{fm}^{-1}$ [21].

The constant Λ in Eq. (1) is scheme dependent quantity. On the lattice it relates to a linear divergence in inverse lattice spacing a^{-1} and in dimensional regularization it manifests as a renor-

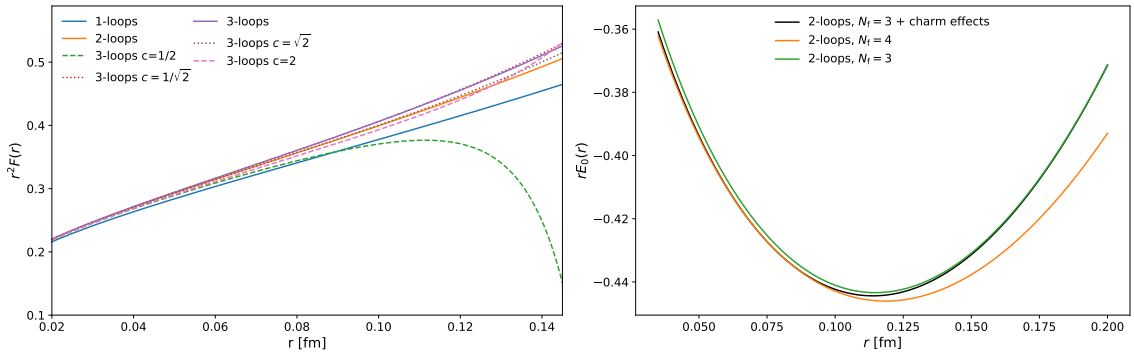

Figure 1: Left: The static force $r^2F(r)$ at different orders of perturbation theory and different scalings of $\mu = c/r$. Right: The static energy at different combinations of light and massive quarks. The free constant shift Λ is optimized to minimize the covered range in y-axis to make the differences between curves more visible.

malon of mass dimension one. Since the constant by itself does not depend on α_s, and all α_s dependence is contained in the r-dependent part of $E_0(r)$, we can obtain α_s from the lattice data by simply matching the lattice results and perturbative curves at some reference distance r^*. However, in order to get as stable as possible perturbative behavior, the issue with renormalon needs to be solved. We explore two strategies to deal with the renormalon contribution:

1. The static force $F(r)$, defined as a derivative with respect to r of the static energy, no longer contains the constant Λ. $F(r)$ can be computed directly on the lattice [10, 25] and compared to perturbative expansion of the static force to extract α_s. However, since we have computed the static energy on the lattice, we take a different approach and integrate the perturbative static force as described in [15, 17] to get more stable definition of $E_0(r)$. The constant Λ reappears, now as an integration constant, and can be matched to lattice data at distance r^*. The total static energy with the finite mass correction then takes the form:

$$E_{0,m}^{(N_f)}(r) = \int_{r^*}^{r} \mathrm{d}r' \;\; F^{(N_f)}(r') + \delta V_m^{(N_f)}(r) + \text{const}\,, \tag{2}$$

   where $N_f = 3$ is the number of massless quarks. In the limit $m \gg 1/r$, Eq. (2) reduces to the case of N_f massless quarks $E_0^{(N_f)}(r)$, while in the limit $m \ll 1/r$ it reduces to case of $N_f + 1$ massless quarks $E_0^{(N_f+1)}(r)$. This is a consequence of the decoupling of charm quark in the static potential. We demonstrate the entire procedure in figure 1. On the left side, we show the static force multiplied by squared distance $r^2F(r)$ at different orders of perturbation theory and at different renormalization scales $\mu = c/r$. On the right side, we show the effect of the charm quark after the force has been integrated back to static energy.

2. Alternatively, we can inspect the minimal renormalon subtraction (MRS) prescription [26–28]. In this method the leading factorial growth of the expansion coefficients is summed to all orders, which stabilizes the behavior of Λ and reduces the perturbative error of the fits. This approach avoids the need to numerically integrate the static force. To deal with the charm sea, we add the correction $\delta V_m^{(N_f)}(r)$ at fixed order to the MRS description of $E_0(r)$.

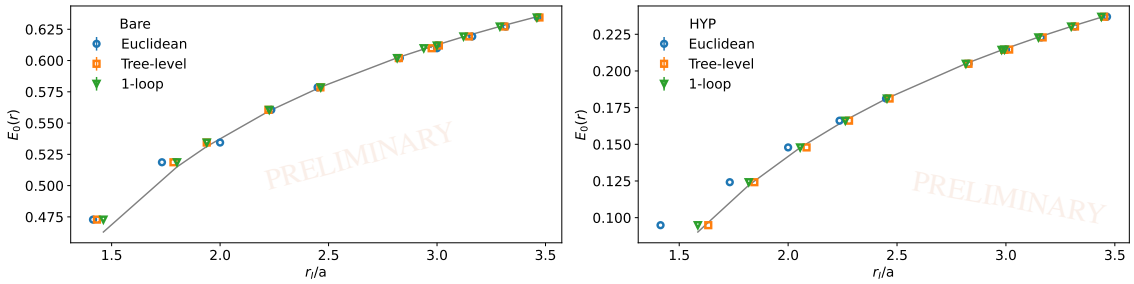

Figure 2: Different orders of improved distance r_I applied to the finest lattice ensemble for the bare (Left) and HYP-smeared (right) $E_0(r)$. The black curve shows a coulombic trend line with fixed coupling.

2.2 Lattice

We compute the static energy from the (2+1+1)-flavor lattice ensembles generated by the MILC Collaboration [29–31]. For gluons the one-loop Symanzik-improved action with tadpole improvement has been used. The sea quarks, namely two isospin-symmetric light quarks, and physical strange and charm quarks, are simulated with the HISQ-action [32]. While the total dataset spans lattice spacings from 0.032 fm to 0.15 fm with light quark mass m_l/m_s being either $1/10$, $1/5$ or physical, in these proceedings we mainly focus on the finest lattice with lattice spacing $a = 0.03216$ fm and $m_l/m_s = 1/5$. Analysis for many of the coarser ensembles and the continuum extrapolation is left for the final publication.

The gauge configurations have been fixed to Coulomb gauge, which allows for easy access to off-axis distances. Instead of the Wilson loops, in Coulomb gauge, $E_0(r)$ can be obtained from the time dependence of the Wilson-line correlation function $C(\boldsymbol{r}, \tau, a)$ at separation $\boldsymbol{r}/a$:

$$\begin{aligned} C(\boldsymbol{r}, \tau, a) &= \left\langle \frac{1}{N_\mathrm{s}^3} \sum_{\boldsymbol{x}} \sum_{\boldsymbol{y}=R(\boldsymbol{r})} \frac{1}{N_\mathrm{c}\, N_{\boldsymbol{r}}} \operatorname{tr}\left[W^\dagger(\boldsymbol{x}+\boldsymbol{y}, \tau, a)\, W(\boldsymbol{x}, \tau, a) \right] \right\rangle \\ &= \sum_{n=0}^{\infty} C_n(\boldsymbol{r}, a) \left(\mathrm{e}^{-\tau E_n(\boldsymbol{r},a)} + \mathrm{e}^{-(aN_\mathrm{t}-\tau)E_n(\boldsymbol{r},a)} \right) \\ &= \mathrm{e}^{-\tau E_0(\boldsymbol{r},a)} \left(C_0(\boldsymbol{r}, a) + \sum_{n=1}^{N_\mathrm{st}-1} C_n(\boldsymbol{r}, a) \prod_{m=1}^{n} \mathrm{e}^{-\tau \Delta_m(\boldsymbol{r},a)} \right) + \ldots, \end{aligned} \tag{3}$$

where we have reparameterized the correlation in terms of energy differences $a\Delta_n(\boldsymbol{r}, a) = aE_n(\boldsymbol{r}, a) - aE_{(n-1)}(\boldsymbol{r}, a) > 0$. We choose $N_\mathrm{st} = 1$, 2, or 3 to fit our data to this form using Bayesian priors and extract $E_0(r)$. The reader is referred to our previous publication for further technical details [33] of the procedure. In Ref. [33], we determined the potential scales r_i, especially $r_1 \simeq 0.3$ fm [34] which is defined from the static force as $r_1^2 F(r_1) = 1$. We will use the r_1-scale as our main scale for the $\Lambda_{\overline{\mathrm{MS}}}$ extraction. The conversion of the results from r_1-units to physical units is discussed further in section 3.1.

After the static energy has been computed, we correct for the discretization artifacts. At short distances of the order of the lattice spacing a, the static energy exhibits significant non-smooth discretization errors. These cutoff effects are known at the leading order and can be removed with a so called tree-level improvement prescription, where an improved distance r_I is defined such that the

continuum and lattice perturbation theories match at leading order. While tree-level improvement allows one to reach shorter distances more smoothly than plain Euclidean r/a, it is not enough for the few first separations. To extend the improvement to even shorter distances, we have performed a rigorous lattice perturbation theory calculation at next-to-leading order (one loop) [35]. The lattice perturbation theory calculation is performed numerically with the `HiPPy` and `HPsrc` packages [36]. The effect of the different levels of improvement is demonstrated in figure 2 where the improvement is shown for both bare or HYP-smeared [37] static quarks. In the figure, one can see that in the bare data for the two distinct path topologies at $r = 3 = \sqrt{3^2} = \sqrt{3^2+0^2+0^2}$ or $= \sqrt{2^2+2^2+1^2}$, the one-loop correction is clearly making the overall shape smoother. The biggest correction from the one-loop improvement compared to the tree-level improvement happens at these on-axis path topologies where the Wilson lines are separated in single cardinal direction. The one-loop calculation in Ref. [35] is still being finalized, and for these proceedings we stick with the tree-level improvement. To compensate for the missing 1-loop effects, we add 0.1% error as an extra systematics to all points $r^2 \leq 8a$, and to further reduce the unwanted discretization effects, we exclude the on-axis points from any of the fits.

3. Extraction of $\Lambda_{\overline{\text{MS}}}$

To extract $\Lambda_{\overline{\text{MS}}}$, we perform a two parameter fit to the perturbative descriptions arising from the two approaches we use to regulate the renormalons. The first fitted parameter is a shift constant Λ that matches the perturbative curve to the lattice data at some distance r^*. Secondly, we fit $\Lambda_{\overline{\text{MS}}}$ that enters the equation (2) via $\alpha_s(\mu = 1/r, \Lambda_{\overline{\text{MS}}})$. The running of the coupling is handled by the `RunDec` [38] library with matching order of power counting to the static potential expansion.

The perturbative formulas describe the non-perturbative lattice data only up to some distances. From previous TUMQCD extractions of $\Lambda_{\overline{\text{MS}}}$ [14, 15, 17], we know that the perturbation theory works well up to ~ 0.13 fm. However, since the charm quark decouples around 0.15 fm, the behavior at 0.13 fm can already be affected by finite mass effects. Therefore, we perform two types of fits. Firstly, we restrict to very short distances $r_{\text{max}} \simeq 0.1$ fm and perform a fit with 4 massless quarks to extract $\Lambda^{(4)}_{\overline{\text{MS}}}$. The caveat of this approach is that we are now more susceptible to the discretization errors. Secondly, we include the charm quark effects to the fit function, as described above, and fit up to separations $r_{\text{max}} = 0.13$ fm with three massless quarks and one heavy quark to extract $\Lambda^{(3)}_{\overline{\text{MS}}}$. The caveat of this approach is that the finite mass effects are known only up to two loops which restricts the entire analysis to two loop accuracy. The third option would be to fit at large distances with 3 massless quarks, but for this to work we would need to fit in range $\gtrsim 0.18$ fm which is clearly out of the perturbative range and hence not considered. The Lambda parameters with different number of fermions $\Lambda^{(N_f)}_{\overline{\text{MS}}}$ can be related to each other by perturbative decoupling relations. For consistency, and for easy comparison with the previous TUMQCD 2+1-flavor extractions, we present all the results as $\Lambda^{(3)}_{\overline{\text{MS}}}$ in these proceedings

With these limits, we perform correlated fits to data divided into 100 jackknife blocks and fit to all possible ranges $a < r_{\text{min}} \leq r \leq r_{\text{max}}$ that have at least three data points. The fits from different ranges are then combined with a model average using the Akaike information criterion (AIC) to weigh the different fits [39]. Since only small fractions of the fits have non-zero AIC weight and

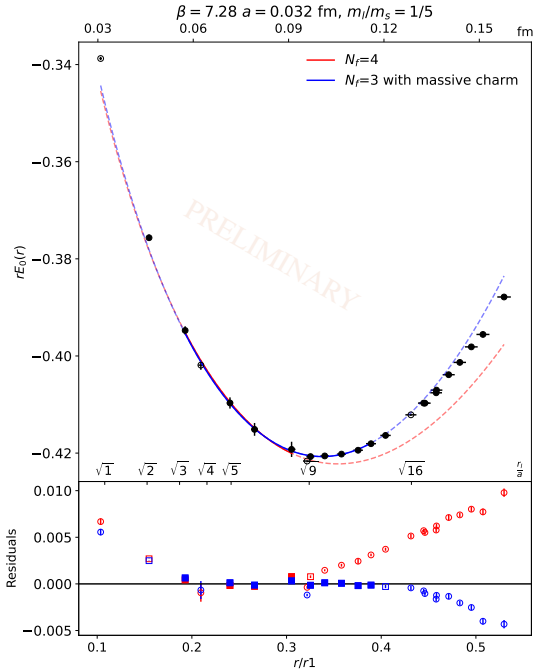

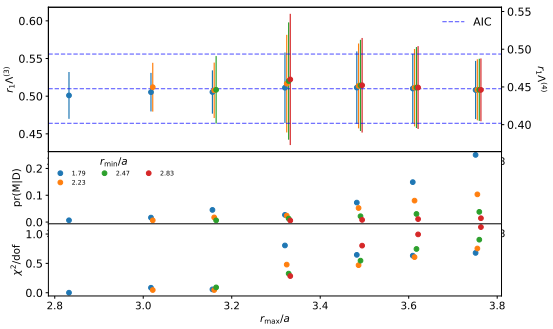

Figure 3: Left: Comparison of the lattice data to the perturbative curves with the fitted $\Lambda_{\overline{\text{MS}}}$. Right: the fit results for individual choices of r_{min} and r_{max} for the 3 flavor + charm fit (blue curve on the left) together with the model weights and χ^2/d.o.f

since these ranges tend to be same between different jackknife blocks, we make sure to use the same set of selected fit ranges for all jackknife blocks.

This fit procedure is demonstrated for the finest ensemble in figure 3. The black points show the lattice data, with the filled points being included in the fit and the empty on-axis point being excluded. The two curves present the fits either with or without the massive charm effects and the solid region represents the range of the fit with best AIC weight. Similarly, on the bottom half of the figure, the filled points correspond to the solid sections of respective lines from above. We observe that the fits describe the data well within the range. Apart from doing the fits with $N_{\text{f}} = 4$ and $N_{\text{f}} = 3 + 1$ flavors, we also repeat the analysis with different orders of the perturbative expansion of the static energy and using both renormalon removal methods. A collection of these fit results for the finest ensemble is shown on the left side of figure 4. Since the finite mass corrections are known only at two-loop level, the extraction with the three-loop static energy with massive charm is incomplete at three loops. Nevertheless, we observe stability between all fit options and general agreement with previous TUMQCD 2+1-flavor extractions [14, 15, 17] and the most recent FLAG average [21].

The fit is then repeated for different scaling factors c of the soft scale $\mu = c/r$. Ideally, one would vary the scale by a factor of two. However, as can be seen from the left of figure 1, the scale variation $c = 1/2$ will heavily constraint the available r-values for the fit. Therefore, at the time of the conference, we could only afford to vary the scale within a more relaxed range $c \in \{1/\sqrt{2}, \sqrt{2}\}$, due to the limited range in r and from the missing one-loop improvement. Moreover, the fit is then repeated over all ensembles. Again, due to available fit ranges with the chosen range of scale variation c, we could only extract $\Lambda_{\overline{\text{MS}}}$ at three finest lattice spacings with a few different light quark masses. Using the $N_{\text{f}} = 3 + 1$ two-loop MRS fit as a reference, we show the lattice spacing dependence of the extracted $\Lambda^{(3)}_{\overline{\text{MS}}}$ on the right side of figure 4, where the points that are grouped together have the same lattice spacing a but different light quark mass ratio m_l/m_s. We observe

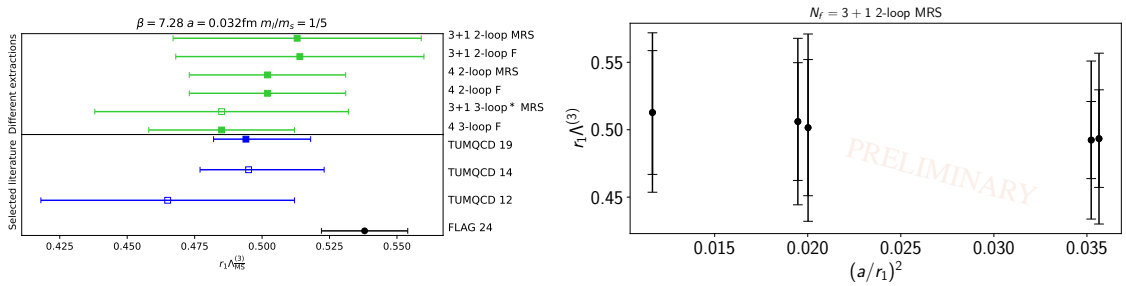

Figure 4: Left: Resulting $r_1\Lambda_{\overline{\rm MS}}$ from the fits to the finest lattice ensemble at different orders of perturbative expansion in green. The 3-loop* point is incomplete at three loops. In blue we show the previous TUMQCD extractions from 2+1 flavors and in black the current FLAG average. The FLAG point is calculated from their $r_0\Lambda$ by multiplying it by the FLAG reported ratio r_1/r_0. Right: One of the fits from the left hand side figure performed to coarser ensembles. The points close to each other have the same lattice spacing (shifted for visibility) but different light quark mass. The inner error bar indicates the statistical error, while the outer error bar shows the systematic error from the variation of the soft scale $\mu = 1/r$ by a factor of $\sqrt{2}$.

mild dependency on the lattice spacing and light quark masses, however, the proper continuum extrapolation is left for future publication. As the results in these proceedings are not final, we only present them in visualized form and refrain from giving quotable numbers until the final publication. Once the $\Lambda_{\overline{\rm MS}}$-parameter has been determined, we can use `RunDec` to obtain the strong coupling at the Z-pole mass $\alpha_{\rm s}(M_{\rm Z})$.

3.1 Physical scale

In these proceedings we decided to present results in r_1-units. In order to convert to physical units, we can use our scale determination [33] $r_1 = 0.3037(25)$ fm, which is based on the $a_{f_{p4s}}$ quantity discussed in Ref. [30]. The previous TUMQCD extraction with 2+1-flavors [17] used a different value for the scale: $r_1 = 0.3106(17)$ fm based on f_π scale. This means that if the comparison on the left side of figure 4 was presented in physical units, there would be slightly more pronounced difference between the $\Lambda^{(3)}_{\rm MS}$ extracted from the (2+1+1)- or (2+1)-flavor datasets. In an upcoming study [40], a new determination of (2+1)-flavor r_1 will be presented based on the Kaon decay constant $f_{\rm K}$. This new constant moves the r_1 value closer to the (2+1+1)-flavor r_1 by a few standard deviations. In general, one does not expect there to be significant finite mass effects in the r_1 scale and hence the three and four flavor physical scales should be close to each other.

Acknowledgments

The lattice QCD calculations have been performed using the publicly available MILC code. The simulations were carried out on the computing facilities of the Computational Center for Particle and Astrophysics (C2PAP) in the project *Calculation of finite T QCD correlators* (pr83pu) and of the SuperMUC cluster at the Leibniz-Rechenzentrum (LRZ) in the project *The role of the charm-quark for the QCD coupling constant* (pn56bo), both located in Munich (Germany), The authors acknowledge the Gauss Centre for Supercomputing e.V. (www.gauss-centre.eu) for funding this project by providing computing time on the GCS Supercomputer SuperMUC-NG at Leibniz Supercomputing Centre (www.lrz.de). This research was funded by the Deutsche Forschungsgemeinschaft

(DFG, German Research Foundation) cluster of excellence "ORIGINS" (www.origins-cluster.de) under Germany's Excellence Strategy EXC-2094-390783311. J.H.W.'s research has been funded by the Deutsche Forschungsgemeinschaft (DFG, German Research Foundation)—Projektnummer 417533893/GRK2575 "Rethinking Quantum Field Theory". The authors acknowledge the support by the State of Hesse within the Research Cluster ELEMENTS (Project ID 500/10.006) N. B. acknowledges the European Research Council advanced grant ERC-2023-ADG-Project EFT-XYZ. P.P. was supported by The U.S. Department of Energy through Contract No. DE-SC0012704. A. B.'s work was supported by the US National Science Foundation under grant No. PHY23-09946. This document was prepared by TUMQCD using the resources of the Fermi National Accelerator Laboratory (Fermilab), a U.S. Department of Energy, Office of Science, Office of High Energy Physics HEP User Facility. Fermilab is managed by Fermi Forward Discovery Group, LLC, acting under Contract No. 89243024CSC000002.

References

[1] G. S. Bali, *QCD forces and heavy quark bound states*, *Phys. Rept.* **343** (2001) 1 [hep-ph/0001312].

[2] N. Brambilla, A. Pineda, J. Soto and A. Vairo, *The infrared behavior of the static potential in perturbative QCD*, *Phys. Rev. D* **60** (1999) 091502 [hep-ph/9903355].

[3] A. Pineda and J. Soto, *The renormalization group improvement of the QCD static potentials*, *Phys. Lett. B* **495** (2000) 323 [hep-ph/0007197].

[4] N. Brambilla, X. Garcia i Tormo, J. Soto and A. Vairo, *The logarithmic contribution to the QCD static energy at N^4LO*, *Phys. Lett. B* **647** (2007) 185 [hep-ph/0610143].

[5] N. Brambilla, A. Vairo, X. Garcia i Tormo and J. Soto, *The QCD static energy at N^3LL*, *Phys. Rev. D* **80** (2009) 034016 [0906.1390].

[6] C. Anzai, Y. Kiyo and Y. Sumino, *Static QCD potential at three-loop order*, *Phys. Rev. Lett.* **104** (2010) 112003 [0911.4335].

[7] A. V. Smirnov, V. A. Smirnov and M. Steinhauser, *Three-loop static potential*, *Phys. Rev. Lett.* **104** (2010) 112002 [0911.4742].

[8] N. Brambilla, X. Garcia i Tormo, J. Soto and A. Vairo, *Precision determination of $r_0\Lambda_{\overline{\rm MS}}$ from the QCD static energy*, *Phys. Rev. Lett.* **105** (2010) 212001 [1006.2066].

[9] N. Husung, M. Koren, P. Krah and R. Sommer, *SU(3) Yang Mills theory at small distances and fine lattices*, *EPJ Web Conf.* **175** (2018) 14024 [1711.01860].

[10] N. Brambilla, V. Leino, J. Mayer-Steudte and A. Vairo, *Static force from generalized Wilson loops on the lattice using the gradient flow*, *Phys. Rev. D* **109** (2024) 114517 [2312.17231].

[11] ETM collaboration, K. Jansen, F. Karbstein, A. Nagy and M. Wagner, *$\Lambda_{\overline{\rm MS}}$ from the static potential for QCD with $n_f = 2$ dynamical quark flavors*, *JHEP* **01** (2012) 025 [1110.6859].

[12] F. Karbstein, A. Peters and M. Wagner, *$\Lambda_{\overline{\rm MS}}^{(n_f=2)}$ from a momentum space analysis of the quark-antiquark static potential*, *JHEP* **09** (2014) 114 [1407.7503].

[13] F. Karbstein, M. Wagner and M. Weber, *Determination of $\Lambda_{\overline{MS}}^{(n_f=2)}$ and analytic parametrization of the static quark-antiquark potential*, *Phys. Rev. D* **98** (2018) 114506 [1804.10909].

[14] A. Bazavov, N. Brambilla, X. Garcia i Tormo, P. Petreczky, J. Soto and A. Vairo, *Determination of α_s from the QCD static energy*, *Phys. Rev. D* **86** (2012) 114031 [1205.6155].

[15] A. Bazavov, N. Brambilla, X. Garcia i Tormo, P. Petreczky, J. Soto and A. Vairo, *Determination of α_s from the QCD static energy: An update*, *Phys. Rev. D* **90** (2014) 074038 [1407.8437].

[16] H. Takaura, T. Kaneko, Y. Kiyo and Y. Sumino, *Determination of α_s from static QCD potential: OPE with renormalon subtraction and lattice QCD*, *JHEP* **04** (2019) 155 [1808.01643].

[17] TUMQCD collaboration, A. Bazavov, N. Brambilla, X. Garcia i Tormo, P. Petreczky, J. Soto, A. Vairo et al., *Determination of the QCD coupling from the static energy and the free energy*, *Phys. Rev. D* **100** (2019) 114511 [1907.11747].

[18] C. Ayala, X. Lobregat and A. Pineda, *Determination of $\alpha(M_Z)$ from an hyperasymptotic approximation to the energy of a static quark-antiquark pair*, *JHEP* **09** (2020) 016 [2005.12301].

[19] ETM collaboration, B. Blossier, P. Boucaud, M. Brinet, F. De Soto, V. Morenas, O. Pene et al., *High statistics determination of the strong coupling constant in Taylor scheme and its OPE Wilson coefficient from lattice QCD with a dynamical charm*, *Phys. Rev. D* **89** (2014) 014507 [1310.3763].

[20] HPQCD collaboration, B. Chakraborty, C. T. H. Davies, B. Galloway, P. Knecht, J. Koponen, G. C. Donald et al., *High-precision quark masses and QCD coupling from $N_f = 4$ lattice QCD*, *Phys. Rev. D* **91** (2015) 054508 [1408.4169].

[21] Flavour Lattice Averaging Group (FLAG) collaboration, Y. Aoki et al., *FLAG Review 2024*, 2411.04268.

[22] D. d'Enterria et al., *The strong coupling constant: State of the art and the decade ahead*, *J. Phys. G* **51** (2024) 090501 [2203.08271].

[23] X. Garcia i Tormo, *Review on the determination of α_s from the QCD static energy*, *Mod. Phys. Lett. A* **28** (2013) 1330028 [1307.2238].

[24] S. Recksiegel and Y. Sumino, *Perturbative QCD potential, renormalon cancellation and phenomenological potentials*, *Phys. Rev. D* **65** (2002) 054018 [hep-ph/0109122].

[25] N. Brambilla, V. Leino, O. Philipsen, C. Reisinger, A. Vairo and M. Wagner, *Lattice gauge theory computation of the static force*, *Phys. Rev. D* **105** (2022) 054514 [2106.01794].

[26] TUMQCD collaboration, N. Brambilla, J. Komijani, A. S. Kronfeld and A. Vairo, *Relations between heavy-light meson and quark masses*, *Phys. Rev. D* **97** (2018) 034503 [1712.04983].

[27] J. Komijani, *A discussion on leading renormalon in the pole mass*, *JHEP* **08** (2017) 062 [1701.00347].

[28] A. S. Kronfeld, *Factorial growth at low orders in perturbative QCD: control over truncation uncertainties*, *JHEP* **12** (2023) 108 [2310.15137].

[29] MILC collaboration, A. Bazavov et al., *Scaling studies of QCD with the dynamical HISQ action*, *Phys. Rev. D* **82** (2010) 074501 [1004.0342].

[30] MILC collaboration, A. Bazavov et al., *Lattice QCD ensembles with four flavors of highly improved staggered quarks*, *Phys. Rev. D* **87** (2013) 054505 [1212.4768].

[31] Fermilab Lattice, MILC collaboration, A. Bazavov et al., *B- and D-meson leptonic decay constants from four-flavor lattice QCD*, *Phys. Rev. D* **98** (2018) 074512 [1712.09262].

[32] HPQCD collaboration, E. Follana, Q. Mason, C. Davies, K. Hornbostel, G. P. Lepage, J. Shigemitsu et al., *Highly improved staggered quarks on the lattice, with applications to charm physics*, *Phys. Rev. D* **75** (2007) 054502 [hep-lat/0610092].

[33] TUMQCD collaboration, N. Brambilla, R. L. Delgado, A. S. Kronfeld, V. Leino, P. Petreczky, S. Steinbeißer et al., *Static energy in (*2 + 1 + 1*)-flavor lattice QCD: Scale setting and charm effects*, *Phys. Rev. D* **107** (2023) 074503 [2206.03156].

[34] C. W. Bernard, T. Burch, K. Orginos, D. Toussaint, T. A. DeGrand, C. E. DeTar et al., *Static quark potential in three-flavor QCD*, *Phys. Rev. D* **62** (2000) 034503 [hep-lat/0002028].

[35] G. M. von Hippel, V. Leino and S. Steinbeißer, *One loop improvement of the static potential with HISQ quarks*, *In preparation: TUM-EFT 171/22* (2025) .

[36] A. Hart, G. M. von Hippel, R. R. Horgan and E. H. Muller, *Automated generation of lattice QCD feynman rules*, *Comput. Phys. Commun.* **180** (2009) 2698 [0904.0375].

[37] A. Hasenfratz and F. Knechtli, *Flavor symmetry and the static potential with hypercubic blocking*, *Phys. Rev. D* **64** (2001) 034504 [hep-lat/0103029].

[38] F. Herren and M. Steinhauser, *Version 3 of* `RunDec` *and* `CRunDec`, *Comput. Phys. Commun.* **224** (2018) 333 [1703.03751].

[39] W. I. Jay and E. T. Neil, *Bayesian model averaging for analysis of lattice field theory results*, *Phys. Rev. D* **103** (2021) 114502 [2008.01069].

[40] P. Petreczky and J. H. Weber, *in preparation*, *private communication* (2025) .